

Measurement of Z0-boson production at large rapidities in Pb-Pb collisions at $\sqrt{s_{NN}}=5.02$ TeV

(ALICE Collaboration) Acharya, S.; ...; Antičić, Tome; ...; Erhardt, Filip; ...; Gotovac, Sven; ...; Jerčić, Marko; ...; ...

Source / Izvornik: **Physics Letters B**, 2018, 780, 372 - 383

Journal article, Published version

Rad u časopisu, Objavljena verzija rada (izdavačev PDF)

<https://doi.org/10.1016/j.physletb.2018.03.010>

Permanent link / Trajna poveznica: <https://urn.nsk.hr/urn:nbn:hr:217:123841>

Rights / Prava: [Attribution 4.0 International](#)/[Imenovanje 4.0 međunarodna](#)

Download date / Datum preuzimanja: **2024-10-14**



Repository / Repozitorij:

[Repository of the Faculty of Science - University of Zagreb](#)





Measurement of Z^0 -boson production at large rapidities in Pb–Pb collisions at $\sqrt{s_{NN}} = 5.02$ TeV

ALICE Collaboration*



ARTICLE INFO

Article history:

Received 7 December 2017
 Received in revised form 21 February 2018
 Accepted 2 March 2018
 Available online 6 March 2018
 Editor: L. Rolandi

ABSTRACT

The production of Z^0 bosons at large rapidities in Pb–Pb collisions at $\sqrt{s_{NN}} = 5.02$ TeV is reported. Z^0 candidates are reconstructed in the dimuon decay channel ($Z^0 \rightarrow \mu^+ \mu^-$), based on muons selected with pseudo-rapidity $-4.0 < \eta < -2.5$ and $p_T > 20$ GeV/c. The invariant yield and the nuclear modification factor, R_{AA} , are presented as a function of rapidity and collision centrality. The value of R_{AA} for the 0–20% central Pb–Pb collisions is 0.67 ± 0.11 (stat.) ± 0.03 (syst.) ± 0.06 (corr. syst.), exhibiting a deviation of 2.6σ from unity. The results are well-described by calculations that include nuclear modifications of the parton distribution functions, while the predictions using vacuum PDFs deviate from data by 2.3σ in the 0–90% centrality class and by 3σ in the 0–20% central collisions.

© 2018 The Author(s). Published by Elsevier B.V. This is an open access article under the CC BY license (<http://creativecommons.org/licenses/by/4.0/>). Funded by SCOAP³.

1. Introduction

Z^0 bosons are weakly interacting probes formed early in the evolution of hadronic collisions ($t_f \sim 1/M \ll 0.01$ fm/c), with a typical decay time $t_d \sim 0.1$ fm/c. Their leptonic decays are of particular interest in heavy-ion collisions, since leptons do not interact strongly and their in-medium energy loss by bremsstrahlung is negligible [1]. Z^0 -boson production rates in hadronic collisions are well-understood, and their measurement via leptonic decays therefore serves as a valuable medium-blind reference for hard processes in heavy-ion collisions [2,3].

Z^0 -boson properties have been extensively studied at LEP (CERN), SLC (SLAC), Tevatron (FNAL) and LHC (CERN) in e^+e^- , $p\bar{p}$ and pp collisions [4–15]. Z^0 -boson production in hadronic collisions is well-described by perturbative Quantum Chromodynamics (pQCD) calculations at next-to-next-to-leading order (NNLO) [16,17], and their comparison with data provides constraints on Parton Distribution Functions (PDFs) [18,19]. In heavy-ion collisions, Z^0 -boson production can be affected by initial-state effects. As a result of the different balance of the number of u and d valence quarks in protons and in lead nuclei (isospin), the yield of Z^0 bosons in Pb–Pb collisions at $\sqrt{s_{NN}} = 5.02$ TeV is expected to increase relative to that in pp collisions by 5–8% at large rapidities, and decrease by 3% at central rapidities [20]. Modifications of the PDFs in nuclei (nPDFs) [21–27] introduce a rapidity-dependent change in yield, with a decrease in yield relative to that in pp collisions of 8–15% at large rapidities, corresponding to the Bjorken- x

ranges $x_1 \gtrsim 10^{-1}$ and $x_2 \lesssim 10^{-3}$, and an increase by 3% at central rapidity, corresponding to $x_{1,2} \sim 10^{-2}$ [20,21]. The yield could also depend upon effects such as multiple scattering and medium-induced bremsstrahlung of the initial partons in large nuclei [28].

The ATLAS, ALICE, CMS and LHCb collaborations have reported measurements of W^\pm - and Z^0 -boson production in p–Pb collisions at $\sqrt{s_{NN}} = 5.02$ TeV [29–33], with complementary rapidity coverage. These measurements are well-described by next-to-leading order (NLO) pQCD calculations [20] and by NNLO calculations using the Fully Exclusive W and Z Production code (FEWZ) [34], utilising both nPDFs [32] and vacuum PDFs. The forward–backward asymmetry of W^\pm -boson production suggests the presence of nuclear modification of PDFs [31]. This sensitivity to nuclear effects indicates the need to include these data in the future nPDF fits.

In Pb–Pb collisions, W^\pm - and Z^0 -boson measurements at $\sqrt{s_{NN}} = 2.76$ TeV have been carried out at central rapidity by the ATLAS and CMS collaborations [35–38]. Preliminary Z^0 -boson measurements in Pb–Pb collisions at $\sqrt{s_{NN}} = 5.02$ TeV at central rapidity have also been reported recently by ATLAS [39]. The W^\pm - and Z^0 -boson nuclear modification factor, R_{AA} , defined as the ratio of the yields in Pb–Pb collisions and the cross-section in pp collisions normalised by the nuclear overlap function (T_{AA}), which represents the effective overlap area of the two interacting nuclei [40], is measured to be consistent with unity within uncertainties, with no centrality dependence [37–39].

Measurements at high collision energy and large rapidities are sensitive to low Bjorken- x processes, and are therefore important to further constrain the initial-state effects on electroweak boson production and to establish a reference for medium-sensitive observables.

* E-mail address: alice-publications@cern.ch.

This paper presents the first measurement of Z^0 -boson production in Pb–Pb collisions at $\sqrt{s_{\text{NN}}} = 5.02$ TeV at large rapidities. Opposite-sign muon pairs from Z^0 -boson decays with $2.5 < y < 4.0$ ¹ are measured with the ALICE detector. The yield of $\mu^+\mu^-$ pairs includes contributions from virtual-photon processes and from their interference effects. This measurement probes the nPDFs of large- x valence quarks ($x_1 \gtrsim 10^{-1}$) and low- x sea quarks ($x_2 \lesssim 10^{-3}$) at $Q^2 \sim M_Z^2$. The invariant yields and R_{AA} are reported as a function of rapidity and collision centrality. The results are compared to model calculations including nPDFs. These measurements complement the measurements in p–Pb collisions at $\sqrt{s_{\text{NN}}} = 5.02$ TeV at large rapidities [32,33], providing increased precision and new information on rapidity and centrality dependence. The combination of these results with future W^\pm measurements in a similar kinematic interval will provide constraints on the flavor dependence of nPDFs, in particular the strange quark contribution [21].

This letter is organised as follows: the experimental setup and data sample are described in Sect. 2; the analysis procedure is presented in Sect. 3; the results are presented in Sect. 4; and a summary is given in Sect. 5.

2. Experimental setup and dataset

The ALICE detector is described in detail in Ref. [41]. Z^0 bosons are reconstructed via their muonic decay with the ALICE muon spectrometer, which provides muon trigger, tracking and identification in the pseudo-rapidity range $-4.0 < \eta < -2.5$. The muon spectrometer, as seen from the interaction point, consists of a front absorber of 10 interaction lengths (λ_{int}) thickness, which reduces the contamination of hadrons and muons from the decay of light particles; five tracking stations; an iron absorber with thickness $7.2 \lambda_{\text{int}}$; and two trigger stations. Each tracking station is composed of two planes of multi-wire proportional chambers with cathode-plane readout, while each trigger station consists of two planes of resistive plate chambers. The third tracking station is located inside the gap of a dipole magnet, which provides a 3 T·m magnetic field integral. The muon spectrometer is completed by a beam shield surrounding the beam pipe that protects the apparatus from secondary particles produced in the interaction of large- η primary particles with the pipe itself.

The interaction vertex is reconstructed using the two cylindrical layers of the Silicon Pixel Detector, located at a radial distance of 3.9 and 7.6 cm from the beam axis and covering $|\eta| < 2$ and $|\eta| < 1.4$, respectively. The V0 detector, consisting of two arrays of scintillator counters covering $2.8 < \eta < 5.1$ and $-3.7 < \eta < -1.8$, is used for triggering and evaluation of collision centrality. Finally, the Zero Degree Calorimeter, placed at 112.5 m from the interaction point along the beam line, is used to reject electromagnetic interactions [42].

The dataset used in this analysis consists of Pb–Pb events at $\sqrt{s_{\text{NN}}} = 5.02$ TeV selected with a dimuon trigger that requires the coincidence of a minimum-bias (MB) trigger and a pair of tracks with opposite sign in the muon spectrometer, each with $p_{\text{T}} \gtrsim 1$ GeV/c. The MB trigger is defined by the coincidence of the signals from both arrays of the V0. The MB trigger is fully efficient for events within the 0–90% centrality interval, which are used in this analysis. The muon trigger efficiency has a plateau of about 98% for muons with $p_{\text{T}} > 5$ GeV/c. The resulting efficiency for pairs of opposite-sign muons, with muon $p_{\text{T}} > 20$ GeV/c and

$-4.0 < \eta < -2.5$, is 95%. After all event selection cuts, the dataset corresponds to an integrated luminosity of about $225 \mu\text{b}^{-1}$.

3. Analysis procedure

The procedure for Z^0 -boson signal extraction in this analysis is the same as that used in the analysis of p–Pb collisions at $\sqrt{s_{\text{NN}}} = 5.02$ TeV [32]. Tracks are reconstructed in the muon spectrometer using the algorithm described in Ref. [43]. Tracks are selected for analysis if they have pseudorapidity $-4.0 < \eta < -2.5$ and polar angle $170^\circ < \theta_{\text{abs}} < 178^\circ$, measured at the end of the front absorber. This selection rejects particles that cross the high-density region of the front absorber and undergo significant multiple scattering. Tracks reconstructed in the tracking stations are identified as muons if they match a track segment in the trigger stations, placed downstream the iron wall. The contamination from background tracks that do not point to the interaction vertex is reduced by utilising the product of the momentum and the distance of closest approach to the interaction vertex. This cut removes 88% of all tracks for events in the 0–90% centrality interval, while retaining all signal candidates with negligible residual background contribution.

Only muons with $p_{\text{T}} > 20$ GeV/c are used in this analysis. This selection reduces the contribution of muons from the decay of charm, beauty and low-mass resonances (see below). Z^0 -boson candidates are formed by combining pairs of opposite-sign muons. The candidates are further selected by requiring that their rapidity, calculated using the measured invariant mass, is in the interval $2.5 < y < 4.0$. Fig. 1 presents the $\mu^+\mu^-$ invariant mass distribution in the centrality intervals 0–90% in Fig. 1(a), 0–20% in Fig. 1(b), and 20–90% in Fig. 1(c). The distribution for the 0–90% centrality interval is compared with the result of a Monte Carlo (MC) simulation obtained using the POWHEG [44] event generator paired with PYTHIA 6.4.25 [45] for the parton shower. The propagation of the particles through the detector is simulated with the GEANT3 code [46]. The isospin of the Pb-nucleus is accounted for by a weighted average of neutron and proton interactions, but no modification of the nucleon PDF was applied to account for nuclear effects. The simulations account for variations in the detector response with time and in-situ alignment effects. A data-driven description of the muon momentum resolution is also implemented (see Ref. [32] for details). The shape of the $\mu^+\mu^-$ invariant mass distribution, which is mainly affected by the momentum resolution, is similar in data and MC.

Various background sources contribute to the $\mu^+\mu^-$ invariant mass distribution. Contamination from the decay of $t\bar{t}$ ($t\bar{t} \rightarrow \mu^+\mu^-X$) and τ ($Z^0 \rightarrow \tau\tau \rightarrow \mu^+\mu^-X$) pairs is estimated with POWHEG simulations [10,44,47] and found to be smaller than 0.5% of the signal yield, which is considered as a systematic uncertainty. The contribution of opposite-sign muon pairs from the decay of $c\bar{c}$ ($c\bar{c} \rightarrow \mu^+\mu^-X$) and $b\bar{b}$ ($b\bar{b} \rightarrow \mu^+\mu^-X$) pairs was studied in p–Pb collisions [32] and found to be smaller than that of $t\bar{t}$ and τ pairs. In Pb–Pb collisions, the presence of high- p_{T} muons from the decay of heavy-flavour pairs is expected to be further reduced due to the in-medium energy loss of heavy quarks. This contribution was therefore neglected. Finally, the combinatorial contribution from the random pairing of muons in the event is evaluated via like-sign muon pairs ($\mu^\pm\mu^\pm$). This combinatorial contribution is found to be small (one candidate in the 20–90% centrality interval) and is subtracted from the signal estimate.

The number of Z^0 candidates is estimated using the procedure described in Ref. [32], by counting the entries in the $\mu^+\mu^-$ invariant mass interval $60 < M_{\mu\mu} < 120$ GeV/c² after subtracting the contribution from like-sign pairs for each centrality and rapidity interval. A total of 64 candidates is found in the 0–90%

¹ In the ALICE reference frame the muon spectrometer covers a negative η range and, consequently, a negative y range. However, since the Pb–Pb system is symmetric in rapidity, a positive y notation is used to present the results.

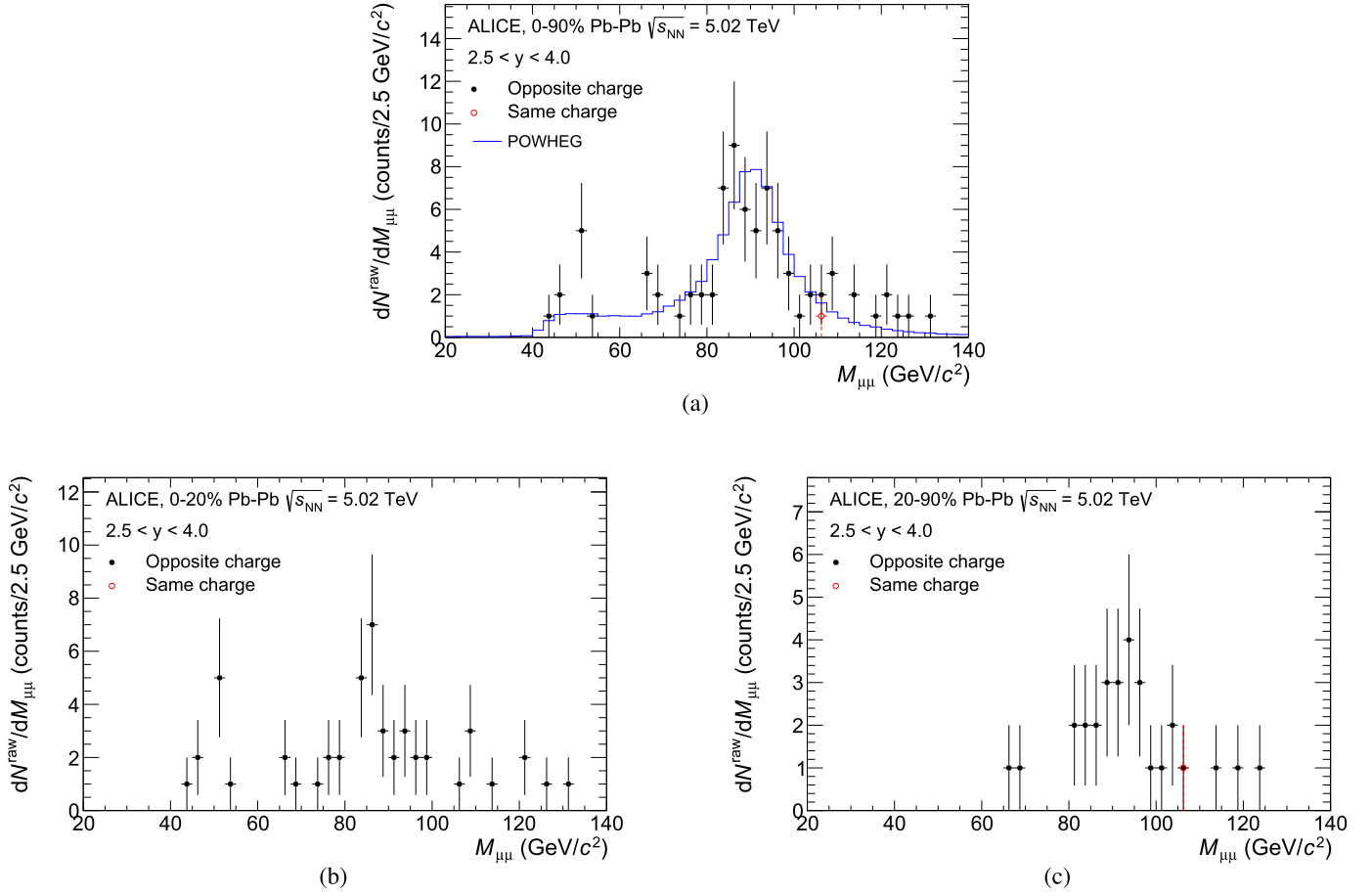


Fig. 1. Invariant mass distribution of $\mu^+ \mu^-$ pairs for Pb–Pb collisions at $\sqrt{s_{NN}} = 5.02$ TeV, reconstructed using muons with $-4.0 < \eta < -2.5$ and $p_T > 20$ GeV/c (black points). The panels present the distribution in different centrality intervals. The error bars are of statistical origin only. The invariant mass distribution of like-sign muon pairs is also shown (red open points). Only one like-sign candidate is found in the 20–90% centrality interval. The solid blue line drawn in Fig. 1(a) represents the distribution from a POWHEG simulation for Pb–Pb collisions without nuclear modification of PDFs (see text for details). (For interpretation of the colours in the figure(s), the reader is referred to the web version of this article.)

centrality bin, of which 37 are in the 0–20% bin and 27 in the 20–90% bin. As a function of rapidity, 33 candidates are in the interval $2.5 < y < 3.0$, and 31 are in the interval $3.0 < y < 4.0$. The raw yields are corrected for the detector acceptance and for reconstruction and selection efficiency ($A \cdot \varepsilon$). The value of $A \cdot \varepsilon$ is 75% for events in the 0–90% centrality interval, estimated using the POWHEG [44] simulations described previously. The dependence of the efficiency on the detector occupancy was evaluated by embedding the generated Z^0 signal in real MB Pb–Pb data. The $A \cdot \varepsilon$ term is constant as a function of centrality from peripheral to semi-central events and decreases in the most central collisions. The value of $A \cdot \varepsilon$ is 78% in the 20–90% centrality interval and 74% in the 0–20% interval, with centrality-independent systematic uncertainty of 5%, as discussed below.

To evaluate the invariant yields (dN/dy), the raw dimuon-triggered mass distribution must be normalised by the factor $F_{\mu\text{-trig}/\text{MB}}^i$, which is the inverse of the probability to observe a dimuon pair in a MB event for the centrality class i . The value of $F_{\mu\text{-trig}/\text{MB}}^i$ is calculated in two different ways, by applying the dimuon selection criterion to MB events, and by the relative counting rate of the two triggers [48]. The variation in $F_{\mu\text{-trig}/\text{MB}}^i$ determined by these two methods is 0.5% and contributes to the systematic uncertainty.

The nuclear modification factor R_{AA} requires the determination of the collision centrality, which is typically quantified by the average number of nucleons participating in the interaction for a given

Table 1

Values of the average nuclear overlap function, $\langle T_{AA} \rangle$, the number of participating nucleons, $\langle N_{\text{part}} \rangle$, and the number of binary nucleon–nucleon collisions, $\langle N_{\text{coll}} \rangle$, for each centrality interval. The average number of participants as weighted by the average number of collisions, $\langle N_{\text{part}} \rangle / \langle N_{\text{coll}} \rangle$, is also reported.

Centrality	$\langle T_{AA} \rangle$ (mb^{-1})	$\langle N_{\text{part}} \rangle$	$\langle N_{\text{coll}} \rangle$	$\langle N_{\text{part}} \rangle / \langle N_{\text{coll}} \rangle$
0–90%	6.2 ± 0.2	126 ± 2	435 ± 41	263 ± 3
0–20%	18.8 ± 0.6	311 ± 3	1318 ± 130	322 ± 3
20–90%	2.61 ± 0.09	73 ± 1	183 ± 15	141 ± 2

centrality bin, N_{part} . However, the rate of hard processes is known to scale with the average number of nucleon–nucleon collisions N_{coll} . The average centrality for hard processes is therefore presented as the average number of participant nucleons weighted by the number of collisions $\langle N_{\text{part}} \rangle / \langle N_{\text{coll}} \rangle$. Table 1 shows the estimates of the average nuclear overlap function $\langle T_{AA} \rangle$, the number of participating nucleons $\langle N_{\text{part}} \rangle$ and the number of binary nucleon–nucleon collisions $\langle N_{\text{coll}} \rangle$, which are obtained via a Glauber model fit of the signal amplitude in the two arrays of the V0 detector [49,50]. The resulting $\langle N_{\text{part}} \rangle / \langle N_{\text{coll}} \rangle$ is also shown. The classification of the events in given centrality intervals has an associated uncertainty of 1.5–2.3% (centrality dependent), that was estimated by comparing the number of candidates selected by varying the centrality ranges by $\pm 0.5\%$, to account for the centrality resolution [49,50].

The sources of systematic uncertainties in the yields and R_{AA} are summarised in Table 2. The systematic uncertainty in the track-

Table 2

Relative systematic uncertainties in the yields and R_{AA} . The ranges quoted for $\langle T_{AA} \rangle$ and the centrality limits, represent the uncertainty variation with centrality. The centrality-dependent correlated uncertainties are marked by the symbol (\star), while the uncertainty sources that are correlated as a function of rapidity are indicated by (\diamond).

Source	Relative systematic uncertainty
Background contamination	<1.0%
Tracking efficiency	3.0% (\star)
Trigger efficiency	1.5% (\star)
Tracker/trigger matching	1.0% (\star)
Alignment	3.5% (\star)
$F_{\mu\text{-trig/MB}}$	0.5% ($\star\diamond$)
σ_{pp}	4.5% (\star)
$\langle T_{AA} \rangle$	3.2–3.5% (\diamond)
Centrality limits	1.5–2.3% (\diamond)

ing efficiency is 3%, obtained from the comparison of the efficiency estimated in data and MC by exploiting the redundancy of the tracking chamber information [51]. The systematic uncertainty of the dimuon trigger efficiency is 1.5%, evaluated by propagating the uncertainty of the efficiency of the detection elements, which is estimated from data using the redundancy of the trigger chamber information. In addition, the choice of the χ^2 cut used to match the tracker and trigger tracks introduces 1% uncertainty, obtained from the difference between data and simulation when applying different χ^2 cuts. The uncertainties in the track resolution and alignment are estimated by comparing the $A \cdot \varepsilon$ values obtained with two different simulations. In the full simulation, the alignment is measured using the MILLEPEDE [52] package and the residual misalignment is taken into account. In the fast simulation, the tracker response is based on a parameterisation of the measured resolution of the clusters associated with a track [32]. The resulting systematic uncertainty is 3.5%.

The total systematic uncertainty in the yield and R_{AA} are determined by summing in quadrature the uncertainty from each source, listed in Table 2. All uncertainties except those due to $\langle T_{AA} \rangle$ and the centrality bin boundaries are independent of collision centrality. Correlations in centrality or rapidity of the uncertainties of different sources are indicated in Table 2. The relative systematic uncertainty in the proton–proton reference σ_{pp} , which affects the R_{AA} , corresponds to 4.5% and is estimated by varying the factorization and renormalisation scales and accounting for the uncertainties in the PDFs [20].

4. Results

The invariant yield of $\mu^+ \mu^-$ from Z^0 bosons in $2.5 < y < 4.0$, divided by $\langle T_{AA} \rangle$, is 6.11 ± 0.76 (stat.) ± 0.38 (syst.) pb for the 0–90% centrality interval. The comparison with theoretical calculations at NLO is shown in Fig. 2. The CT14 [53] prediction utilises free proton and neutron PDFs, with relative weights to account for the isospin of the Pb nucleus. The uncertainty on the model include the uncertainty on the NLO calculations and of the measurements considered in the PDF fit. The measured invariant yield deviates from the lower limit of this prediction by 2.3σ . For the description of nuclear PDFs, two different approaches were considered. The standard approach evaluates the nPDF as the free PDF multiplied by a parameterisation of nuclear modifications. The calculations obtained with the EPS09 [54] and the more recent EPPS16 [22] parameterisations are shown. In the other approach, the nPDFs are obtained by fitting the nuclear data in a similar way as done for free proton data, but using a parameterisation that depends on the atomic mass of the nucleus. The results obtained with the nCTEQ15 nuclear PDFs [21,55] are also presented. The

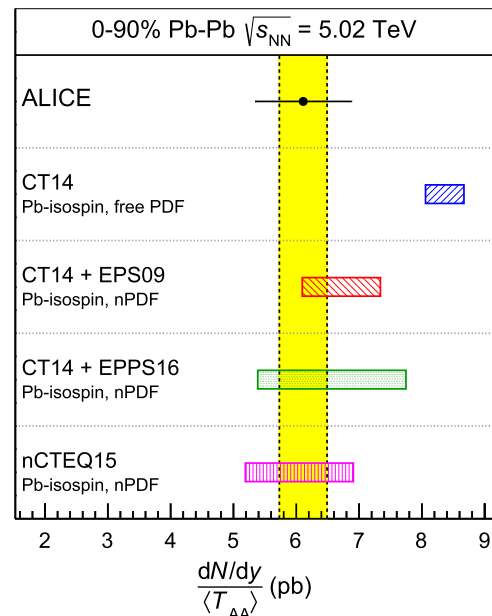


Fig. 2. Invariant yield of $\mu^+ \mu^-$ from Z^0 production in $2.5 < y < 4.0$ divided by the average nuclear overlap function in the 0–90% centrality class, considering muons with $-4.0 < \eta < -2.5$ and $p_T > 20$ GeV/c. The horizontal solid line represents the statistical uncertainty of the measurement while the yellow filled band shows the systematic uncertainty. The result is compared to theoretical calculations with and without nuclear modification of the PDFs [21,22,53–55]. All model calculations incorporate PDFs or nPDFs determined by considering the isospin of the Pb-nucleus.

nPDF sets are characterised by their different approximations and by different input data included in the calculations (see Ref. [22] and references therein for details). Only the most recent EPPS16 parameterisation includes LHC jet, W^\pm and Z^0 data, although the W^\pm and Z^0 data provide only weak constraints on nPDFs at the current perturbative order of the calculation (NLO) [21,56]. In general, the nPDFs have larger uncertainties compared to the free proton PDFs, since they are less constrained from data. CT14+EPS09 and CT14+EPPS16 estimates combine CT14 and EPS09 or EPPS16 uncertainties, whereas nCTEQ15 does a global study of the proton and nuclear measurement uncertainties included in the fit. EPPS16 allows much more freedom for the flavour dependence of nPDFs than other current analyses, which results in larger uncertainties. All pQCD calculations shown in Fig. 2 that use nPDFs describe the measurement well.

The rapidity dependence of the Z^0 -boson invariant yields divided by $\langle T_{AA} \rangle$ is shown in Fig. 3(a). The results are compared to pQCD calculations using the CT14 [53] PDF set both with (green filled box) and without (blue hatched box) the EPPS16 [22] parameterisation of the nPDFs. In both cases, the Pb-isospin effect is modelled by combining the proton and neutron PDFs or nPDFs. EPPS16 decreases the yields but does not have a strong influence on the rapidity dependence of the calculation. The calculations that utilise vacuum PDFs overestimate data in the two rapidity intervals, whereas those that utilise nPDFs are in good agreement with data.

In this analysis, the ratio R_{AA} utilises a theoretically calculated reference cross section for pp collisions [20], which is $\sigma_{pp} = 11.92 \pm 0.43$ pb. The value of R_{AA} for the 0–90% centrality class is determined to be 0.77 ± 0.10 (stat.) ± 0.06 (syst.), deviating by 2.1σ from unity. The pQCD calculation using CT14 [53] and considering only the isospin effects, finds $R_{AA}^{\text{CT14}} = 1.052 \pm 0.038$. The modification of the PDFs in nuclei results in a net reduction of the yields, and consequently in R_{AA} values lower than unity, with $R_{AA}^{\text{CT14+EPPS16}} = 0.845 \pm 0.068$, in agreement with data. The rapid-

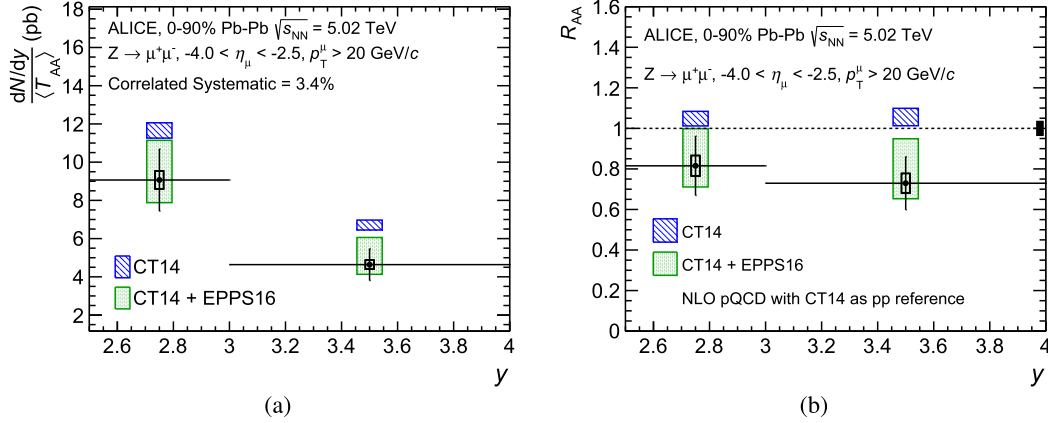


Fig. 3. Invariant yield of $\mu^+ \mu^-$ from Z^0 in $2.5 < y < 4.0$ divided by $\langle T_{AA} \rangle$ (a) and nuclear modification factor (b) as a function of rapidity for Pb-Pb collisions at $\sqrt{s_{NN}} = 5.02$ TeV, considering muons with $-4.0 < \eta < -2.5$ and $p_T > 20$ GeV/c. The vertical error bars are statistical only. The horizontal error bars display the measurement bin width, while the boxes represent the systematic uncertainties. The filled black box in panel (b), located at $R_{AA} = 1$, shows the normalisation uncertainty. The results are compared to theoretical calculations with and without nuclear modification of the PDFs. The filled blue boxes show the calculation using the CT14 PDF, while the green stippled boxes show the calculation using CT14 PDF with EPPS16 nPDFs [22,53]. All model calculations incorporate PDFs or nPDFs that account for the isospin of the Pb nucleus.

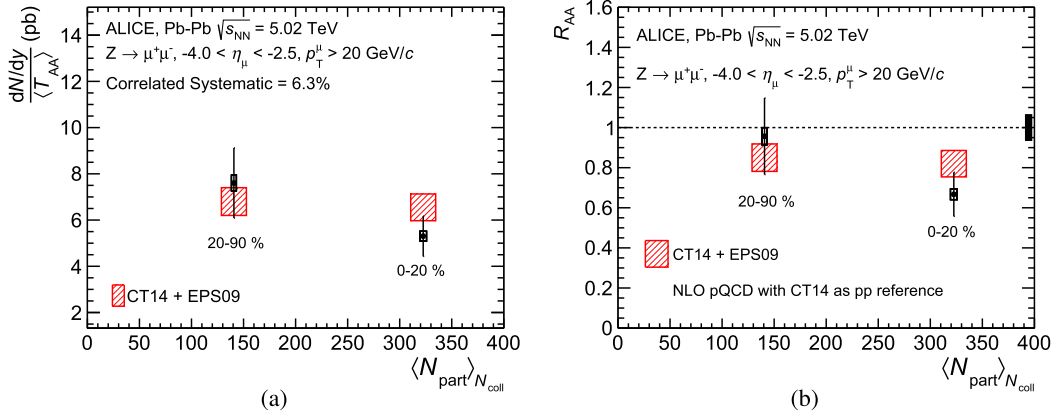


Fig. 4. Invariant yield of $\mu^+ \mu^-$ from Z^0 in $2.5 < y < 4.0$ divided by $\langle T_{AA} \rangle$ (a) and nuclear modification factor (b) as a function of centrality (represented by $\langle N_{part} \rangle_{N_{coll}}$) for Pb-Pb collisions at $\sqrt{s_{NN}} = 5.02$ TeV, considering muons with $-4.0 < \eta < -2.5$ and $p_T > 20$ GeV/c. The vertical error bars are statistical only, while the boxes represent the systematic uncertainties. The filled black box in panel (b), located at $R_{AA} = 1$, shows the normalisation uncertainty. The results are compared to theoretical calculations with centrality-dependent nPDFs that account for the isospin of the Pb nucleus [53,54,57].

ity dependence of R_{AA} is presented in Fig. 3(b). The values are smaller than unity, with a slight rapidity dependence. The data are well-described by calculations including nPDFs (green filled boxes), while the calculations including only isospin effects (blue hatched boxes) tend to overestimate the measured values.

Z^0 -boson production is studied as a function of the collision centrality, expressed in terms of $\langle N_{part} \rangle_{N_{coll}}$ as shown in Fig. 4. The value of R_{AA} is compatible with unity in peripheral collisions, with R_{AA} (20–90%) = 0.96 ± 0.19 (stat.) ± 0.04 (syst.) ± 0.06 (corr. syst.), while it is 2.6σ smaller than unity in the central collisions, with R_{AA} (0–20%) = 0.67 ± 0.11 (stat.) ± 0.03 (syst.) ± 0.04 (corr. syst.). The value for 0–20% central collisions deviates from the predictions using vacuum PDFs (R_{AA}^{CT14}) by 3σ . The data are compared to calculations including a centrality-dependent nuclear modification of the PDFs [57], which describe the data within uncertainties.

5. Conclusion

We have reported the first measurement of Z^0 -boson production at forward rapidities in Pb-Pb collisions at $\sqrt{s_{NN}} = 5.02$ TeV. The invariant yields divided by the average nuclear overlap function are evaluated as a function of rapidity and average number of participant nucleons weighted by the number of binary nucleon-

nucleon collisions. The corresponding values of the nuclear modification factor are estimated by dividing the measured yields in Pb-Pb collisions by the expected cross-section in pp collisions estimated with NLO pQCD calculations. The value of R_{AA} is compatible with unity in the 20–90% centrality class (within large statistical uncertainty), whereas it is smaller than unity by 2.6 times the quadratic sum of the statistical and systematic uncertainties in the 0–20% most central collisions. The results are well-described by the calculations that include modifications of the PDFs in nuclei. In contrast, the calculations with vacuum PDFs overestimate the centrality-integrated R_{AA} by 2.3σ and R_{AA} in the 0–20% most central collisions by 3σ .

Acknowledgements

The ALICE Collaboration would like to thank H. Paukkunen for providing the pQCD calculations with EPS09 and EPPS16, and F. Lyonnet and A. Kusina for providing the pQCD calculations with nCTEQ15.

The ALICE Collaboration would like to thank all its engineers and technicians for their invaluable contributions to the construction of the experiment and the CERN accelerator teams for the outstanding performance of the LHC complex. The ALICE Collab-

oration gratefully acknowledges the resources and support provided by all Grid centres and the Worldwide LHC Computing Grid (WLCG) collaboration. The ALICE Collaboration acknowledges the following funding agencies for their support in building and running the ALICE detector: A.I. Alikhanyan National Science Laboratory (Yerevan Physics Institute) Foundation (ANSL), State Committee of Science and World Federation of Scientists (WFS), Armenia; Austrian Academy of Sciences and Nationalstiftung für Forschung, Technologie und Entwicklung, Austria; Ministry of Communications and High Technologies, National Nuclear Research Center, Azerbaijan; Conselho Nacional de Desenvolvimento Científico e Tecnológico (CNPq), Universidade Federal do Rio Grande do Sul (UFRGS), Financiadora de Estudos e Projetos (Finep) and Fundação de Amparo à Pesquisa do Estado de São Paulo (FAPESP), Brazil; Ministry of Science & Technology of China (MSTC), National Natural Science Foundation of China (NSFC) and Ministry of Education of China (MOEC), China; Ministry of Science, Education and Sports and Croatian Science Foundation, Croatia; Ministry of Education, Youth and Sports of the Czech Republic, Czech Republic; The Danish Council for Independent Research – Natural Sciences, the Carlsberg Foundation and Danish National Research Foundation (DNRF), Denmark; Helsinki Institute of Physics (HIP), Finland; Commissariat à l’Energie Atomique (CEA) and Institut National de Physique Nucléaire et de Physique des Particules (IN2P3) and Centre National de la Recherche Scientifique (CNRS), France; Bundesministerium für Bildung, Wissenschaft, Forschung und Technologie (BMBF) and GSI Helmholtzzentrum für Schwerionenforschung GmbH, Germany; General Secretariat for Research and Technology, Ministry of Education, Research and Religions, Greece; National Research, Development and Innovation Office, Hungary; Department of Atomic Energy, Government of India (DAE), Department of Science and Technology, Government of India (DST), University Grants Commission, Government of India (UGC) and Council of Scientific and Industrial Research (CSIR), India; Indonesian Institute of Science, Indonesia; Centro Fermi – Museo Storico della Fisica e Centro Studi e Ricerche Enrico Fermi and Istituto Nazionale di Fisica Nucleare (INFN), Italy; Institute for Innovative Science and Technology, Nagasaki Institute of Applied Science (IIST), Japan Society for the Promotion of Science (JSPS) KAKENHI and Japanese Ministry of Education, Culture, Sports, Science and Technology (MEXT), Japan; Consejo Nacional de Ciencia (CONACYT) y Tecnología, through Fondo de Cooperación Internacional en Ciencia y Tecnología (FONCICYT) and Dirección General de Asuntos del Personal Académico (DGAPA), Mexico; Nederlandse Organisatie voor Wetenschappelijk Onderzoek (NWO), Netherlands; The Research Council of Norway, Norway; Commission on Science and Technology for Sustainable Development in the South (COMSATS), Pakistan; Pontificia Universidad Católica del Perú, Peru; Ministry of Science and Higher Education and National Science Centre, Poland; Korea Institute of Science and Technology Information and National Research Foundation of Korea (NRF), Republic of Korea; Ministry of Education and Scientific Research, Institute of Atomic Physics and Romanian National Agency for Science, Technology and Innovation, Romania; Joint Institute for Nuclear Research (JINR), Ministry of Education and Science of the Russian Federation and National Research Centre Kurchatov Institute, Russia; Ministry of Education, Science, Research and Sport of the Slovak Republic, Slovakia; National Research Foundation of South Africa, South Africa; Centro de Aplicaciones Tecnológicas y Desarrollo Nuclear (CEADEN), Cubaenergía, Cuba and Centro de Investigaciones Energéticas, Medioambientales y Tecnológicas (CIEMAT), Spain; Swedish Research Council (VR) and Knut & Alice Wallenberg Foundation (KAW), Sweden; European Organization for Nuclear Research, Switzerland; National Science and Technology Development Agency (NSDTA), Suranaree University of Technology (SUT) and Office of the Higher Educa-

tion Commission under NRU project of Thailand, Thailand; Turkish Atomic Energy Agency (TAEK), Turkey; National Academy of Sciences of Ukraine, Ukraine; Science and Technology Facilities Council (STFC), United Kingdom; National Science Foundation of the United States of America (NSF) and United States Department of Energy, Office of Nuclear Physics (DOE NP), United States of America.

References

- [1] S. Peigne, A. Peshier, Collisional energy loss of a fast muon in a hot QED plasma, *Phys. Rev. D* 77 (2008) 014015, arXiv:0710.1266 [hep-ph].
- [2] V. Kartvelishvili, R. Kvatadze, R. Shanidze, On Z and Z + jet production in heavy ion collisions, *Phys. Lett. B* 356 (1995) 589–594, arXiv:hep-ph/9505418.
- [3] Z. Conesa del Valle, Vector bosons in heavy-ion collisions at the LHC, *Eur. Phys. J. C* 61 (2009) 729–733, arXiv:0903.1432 [hep-ex].
- [4] UA1 Collaboration, C. Albajar, et al., Intermediate vector Boson cross-sections at the CERN super proton synchrotron collider and the number of neutrino types, *Phys. Lett. B* 198 (1987) 271.
- [5] UA2 Collaboration, J. Alitti, et al., A Measurement of the W and Z production cross-sections and a determination of Γ_W at the CERN $\bar{p}p$ collider, *Phys. Lett. B* 276 (1992) 365–374.
- [6] CDF Collaboration, F. Abe, et al., Measurement of $\sigma \cdot B(W \rightarrow e\nu)$ and $\sigma \cdot B(Z^0 \rightarrow e^+e^-)$ in $p\bar{p}$ collisions at $\sqrt{s} = 1.8$ TeV, *Phys. Rev. Lett.* 76 (1996) 3070–3075, arXiv:hep-ex/9509010.
- [7] D0 Collaboration, B. Abbott, et al., Extraction of the width of the W boson from measurements of $\sigma(p\bar{p} \rightarrow W+X) \times B(W \rightarrow e\nu)$ and $\sigma(p\bar{p} \rightarrow Z+X) \times B(Z \rightarrow ee)$ and their ratio, *Phys. Rev. D* 61 (2000) 072001, arXiv:hep-ex/9906025.
- [8] CDF Collaboration, A. Abulencia, et al., Measurements of inclusive W and Z cross sections in $p\bar{p}$ collisions at $\sqrt{s} = 1.96$ TeV, *J. Phys. G* 34 (2007) 2457–2544, arXiv:hep-ex/0508029.
- [9] ATLAS Collaboration, G. Aad, et al., Measurement of the $W \rightarrow \ell\nu$ and $Z/\gamma^* \rightarrow \ell\ell$ production cross sections in proton–proton collisions at $\sqrt{s} = 7$ TeV with the ATLAS detector, *J. High Energy Phys.* 12 (2010) 060, arXiv:1010.2130 [hep-ex].
- [10] ATLAS Collaboration, G. Aad, et al., Measurement of the inclusive W^\pm and Z/γ^* cross sections in the electron and muon decay channels in pp collisions at $\sqrt{s} = 7$ TeV with the ATLAS detector, *Phys. Rev. D* 85 (2012) 072004, arXiv:1109.5141 [hep-ex].
- [11] ATLAS Collaboration, G. Aad, et al., Measurement of W^\pm and Z-boson production cross sections in pp collisions at $\sqrt{s} = 13$ TeV with the ATLAS detector, *Phys. Lett. B* 759 (2016) 601–621, arXiv:1603.09222 [hep-ex].
- [12] CMS Collaboration, S. Chatrchyan, et al., Measurement of the inclusive W and Z production cross sections in pp collisions at $\sqrt{s} = 7$ TeV, *J. High Energy Phys.* 10 (2011) 132, arXiv:1107.4789 [hep-ex].
- [13] CMS Collaboration, S. Chatrchyan, et al., Measurement of inclusive W and Z boson production cross sections in pp collisions at $\sqrt{s} = 8$ TeV, *Phys. Rev. Lett.* 112 (2014) 191802, arXiv:1402.0923 [hep-ex].
- [14] LHCb Collaboration, R. Aaij, et al., Measurement of the forward Z boson production cross-section in pp collisions at $\sqrt{s} = 7$ TeV, *J. High Energy Phys.* 08 (2015) 039, arXiv:1505.07024 [hep-ex].
- [15] LHCb Collaboration, R. Aaij, et al., Measurement of forward W and Z boson production in pp collisions at $\sqrt{s} = 8$ TeV, *J. High Energy Phys.* 01 (2016) 155, arXiv:1511.08039 [hep-ex].
- [16] A.D. Martin, R.G. Roberts, W.J. Stirling, R.S. Thorne, Parton distributions and the LHC: W and Z production, *Eur. Phys. J. C* 14 (2000) 133–145, arXiv:hep-ph/9907231.
- [17] U. Baur, S. Keller, D. Wackertho, Electroweak radiative corrections to W boson production in hadronic collisions, *Phys. Rev. D* 59 (1999) 013002, arXiv:hep-ph/9807417.
- [18] J. Rojo, et al., The PDF4LHC report on PDFs and LHC data: results from Run I and preparation for Run II, *J. Phys. G* 42 (2015) 103103, arXiv:1507.00556 [hep-ph].
- [19] J. Butterworth, et al., PDF4LHC recommendations for LHC Run II, *J. Phys. G* 43 (2016) 023001, arXiv:1510.03865 [hep-ph].
- [20] H. Paukkunen, C.A. Salgado, Constraints for the nuclear parton distributions from Z and W production at the LHC, *J. High Energy Phys.* 1103 (2011) 071, arXiv:1010.5392 [hep-ph].
- [21] A. Kusina, F. Lyonnet, D.B. Clark, E. Godat, T. Jezo, K. Kovarik, F.I. Olness, I. Schienbein, J.Y. Yu, Vector boson production in proton–lead and lead–lead collisions at the LHC and its impact on nCTEQ15 PDFs, arXiv:1610.02925 [nucl-th].
- [22] K.J. Eskola, P. Paakkinen, H. Paukkunen, C.A. Salgado, EPPS16: nuclear parton distributions with LHC data, *Eur. Phys. J. C* 77 (2017) 163, arXiv:1612.05741 [hep-ph].
- [23] D. de Florian, R. Sassot, Nuclear parton distributions at next-to-leading order, *Phys. Rev. D* 69 (2004) 074028, arXiv:hep-ph/0311227.

- [24] M. Hirai, S. Kumano, T.H. Nagai, Determination of nuclear parton distribution functions and their uncertainties in next-to-leading order, *Phys. Rev. C* 76 (2007) 065207, arXiv:0709.3038 [hep-ph].
- [25] S. Atashbar Tehrani, Nuclear parton densities and their uncertainties at the next-to-leading order, *Phys. Rev. C* 86 (2012) 064301.
- [26] H. Khanpour, S. Atashbar Tehrani, Global analysis of nuclear parton distribution functions and their uncertainties at next-to-next-to-leading order, *Phys. Rev. D* 93 (2016) 014026, arXiv:1601.00939 [hep-ph].
- [27] R. Vogt, Shadowing effects on vector boson production, *Phys. Rev. C* 64 (2001) 044901, arXiv:hep-ph/0011242.
- [28] R.B. Neufeld, I. Vitev, B.-W. Zhang, A possible determination of the quark radiation length in cold nuclear matter, *Phys. Lett. B* 704 (2011) 590–595, arXiv:1010.3708 [hep-ph].
- [29] ATLAS Collaboration, G. Aad, et al., Z boson production in p + Pb collisions at $\sqrt{s_{NN}} = 5.02$ TeV measured with the ATLAS detector, *Phys. Rev. C* 92 (2015) 044915, arXiv:1507.06232 [hep-ex].
- [30] CMS Collaboration, V. Khachatryan, et al., Study of Z boson production in pPb collisions at $\sqrt{s_{NN}} = 5.02$ TeV, *Phys. Lett. B* 759 (2016) 36–57, arXiv:1512.06461 [hep-ex].
- [31] CMS Collaboration, V. Khachatryan, et al., Study of W boson production in pPb collisions at $\sqrt{s_{NN}} = 5.02$ TeV, *Phys. Lett. B* 750 (2015) 565–586, arXiv:1503.05825 [nucl-ex].
- [32] ALICE Collaboration, J. Adam, et al., W and Z boson production in p-Pb collisions at $\sqrt{s_{NN}} = 5.02$ TeV, *J. High Energy Phys.* 02 (2017) 077, arXiv:1611.03002 [nucl-ex].
- [33] LHCb Collaboration, R. Aaij, et al., Observation of Z production in proton–lead collisions at LHCb, *J. High Energy Phys.* 1409 (2014) 030, arXiv:1406.2885 [hep-ex].
- [34] R. Gavin, Y. Li, F. Petriello, S. Quackenbush, FEWZ 2.0: a code for hadronic Z production at next-to-next-to-leading order, *Comput. Phys. Commun.* 182 (2011) 2388–2403, arXiv:1011.3540 [hep-ph].
- [35] ATLAS Collaboration, G. Aad, et al., Measurement of the production and lepton charge asymmetry of W bosons in Pb+Pb collisions at $\sqrt{s_{NN}} = 2.76$ TeV with the ATLAS detector, *Eur. Phys. J. C* 75 (2015) 23, arXiv:1408.4674 [hep-ex].
- [36] ATLAS Collaboration, G. Aad, et al., Measurement of Z boson Production in Pb+Pb Collisions at $\sqrt{s_{NN}} = 2.76$ TeV with the ATLAS Detector, *Phys. Rev. Lett.* 110 (2013) 022301, arXiv:1210.6486 [hep-ex].
- [37] CMS Collaboration, S. Chatrchyan, et al., Study of Z production in PbPb and pp collisions at $\sqrt{s_{NN}} = 2.76$ TeV in the dimuon and dielectron decay channels, *J. High Energy Phys.* 1503 (2015) 022, arXiv:1410.4825 [nucl-ex].
- [38] CMS Collaboration, S. Chatrchyan, et al., Study of W boson production in PbPb and pp collisions at $\sqrt{s_{NN}} = 2.76$ TeV, *Phys. Lett. B* 715 (2012) 66–87, arXiv:1205.6334 [nucl-ex].
- [39] ATLAS Collaboration, Z boson production in Pb+Pb collisions at $\sqrt{s_{NN}} = 5.02$ TeV with the ATLAS detector at the LHC, ATLAS-CONF-2017-010, 2017.
- [40] M.L. Miller, K. Reygers, S.J. Sanders, P. Steinberg, Glauber modeling in high energy nuclear collisions, *Annu. Rev. Nucl. Part. Sci.* 57 (2007) 205–243, arXiv:nucl-ex/0701025.
- [41] ALICE Collaboration, K. Aamodt, et al., The ALICE experiment at the CERN LHC, *J. Instrum.* 3 (2008) S08002.
- [42] ALICE Collaboration, B. Abelev, et al., Measurement of the cross section for electromagnetic dissociation with neutron emission in Pb–Pb collisions at $\sqrt{s_{NN}} = 2.76$ TeV, *Phys. Rev. Lett.* 109 (2012) 252302, arXiv:1203.2436 [nucl-ex].
- [43] ALICE Collaboration, K. Aamodt, et al., Rapidity and transverse momentum dependence of inclusive J/ψ production in pp collisions at $\sqrt{s} = 7$ TeV, *Phys. Lett. B* 704 (2011) 442–455, arXiv:1105.0380 [hep-ex], Erratum: *Phys. Lett. B* 7 (2012) 18,692.
- [44] S. Alioli, P. Nason, C. Oleari, E. Re, NLO vector-boson production matched with shower in POWHEG, *J. High Energy Phys.* 07 (2008) 060, arXiv:0805.4802 [hep-ph].
- [45] T. Sjostrand, S. Mrenna, P.Z. Skands, PYTHIA 6.4 physics and manual, *J. High Energy Phys.* 05 (2006) 026, arXiv:hep-ph/0603175.
- [46] R. Brun, F. Carminati, S. Giani, GEANT detector description and simulation tool, CERN-W-5013, 1994.
- [47] CMS Collaboration, S. Chatrchyan, et al., Measurement of the rapidity and transverse momentum distributions of Z bosons in pp collisions at $\sqrt{s} = 7$ TeV, *Phys. Rev. D* 85 (2012) 032002, arXiv:1110.4973 [hep-ex].
- [48] ALICE Collaboration, J. Adam, et al., J/ψ suppression at forward rapidity in Pb–Pb collisions at $\sqrt{s_{NN}} = 5.02$ TeV, *Phys. Lett. B* 766 (2017) 212–224, arXiv:1606.08197 [nucl-ex].
- [49] ALICE Collaboration, J. Adam, et al., Centrality dependence of particle production in p–Pb collisions at $\sqrt{s_{NN}} = 5.02$ TeV, *Phys. Rev. C* 91 (2015) 064905, arXiv:1412.6828 [nucl-ex].
- [50] ALICE Collaboration, J. Adam, et al., Centrality dependence of the charged-particle multiplicity density at midrapidity in Pb–Pb collisions at $\sqrt{s_{NN}} = 5.02$ TeV, *Phys. Rev. Lett.* 116 (2016) 222302, arXiv:1512.06104 [nucl-ex].
- [51] ALICE Collaboration, B.B. Abelev, et al., Performance of the ALICE experiment at the CERN LHC, *Int. J. Mod. Phys. A* 29 (2014) 1430044, arXiv:1402.4476 [nucl-ex].
- [52] V. Blobel, C. Kleinwort, A new method for the high precision alignment of track detectors, in: *Advanced Statistical Techniques in Particle Physics. Proceedings, Conference, Durham, UK, March 18–22, 2002, 2002*, pp. URL-STR(9), arXiv:hep-ex/0208021, <http://www.ipp.dur.ac.uk/Workshops/02/statistics/proceedings/blobel1.pdf>, 2002.
- [53] S. Dulat, T.-J. Hou, J. Gao, M. Guzzi, J. Huston, P. Nadolsky, J. Pumplin, C. Schmidt, D. Stump, C.P. Yuan, New parton distribution functions from a global analysis of quantum chromodynamics, *Phys. Rev. D* 93 (2016) 033006, arXiv:1506.07443 [hep-ph].
- [54] K.J. Eskola, H. Paukkunen, C.A. Salgado, EPS09: a new generation of NLO and LO nuclear parton distribution functions, *J. High Energy Phys.* 04 (2009) 065, arXiv:0902.4154 [hep-ph].
- [55] K. Kovarik, et al., nCTEQ15 – global analysis of nuclear parton distributions with uncertainties in the CTEQ framework, *Phys. Rev. D* 93 (2016) 085037, arXiv:1509.00792 [hep-ph].
- [56] N. Armesto, H. Paukkunen, J.M. Penín, C.A. Salgado, P. Zurita, An analysis of the impact of LHC Run I proton–lead data on nuclear parton densities, *Eur. Phys. J. C* 76 (2016) 218, arXiv:1512.01528 [hep-ph].
- [57] I. Helenius, K.J. Eskola, H. Honkanen, C.A. Salgado, Impact-parameter dependent nuclear parton distribution functions: EPS09s and EKS98s and their applications in nuclear hard processes, *J. High Energy Phys.* 07 (2012) 073, arXiv:1205.5359 [hep-ph].

The ALICE Collaboration

S. Acharya¹³⁷, D. Adamová⁹⁴, J. Adolfsson³³, M.M. Aggarwal⁹⁹, G. Aglieri Rinella³⁴, M. Agnello³⁰, N. Agrawal⁴⁷, Z. Ahammed¹³⁷, S.U. Ahn⁷⁸, S. Aiola¹⁴¹, A. Akindinov⁶³, M. Al-Turany¹⁰⁶, S.N. Alam¹³⁷, D.S.D. Albuquerque¹²², D. Aleksandrov⁹⁰, B. Alessandro⁵⁷, R. Alfaro Molina⁷³, Y. Ali¹⁵, A. Alici^{11,26,52}, A. Alkin³, J. Alme²¹, T. Alt⁶⁹, L. Altenkamper²¹, I. Altsybeev¹³⁶, C. Andrei⁸⁷, D. Andreou³⁴, H.A. Andrews¹¹⁰, A. Andronic¹⁰⁶, M. Angeletti³⁴, V. Anguelov¹⁰⁴, C. Anson⁹⁷, T. Antičić¹⁰⁷, F. Antinori⁵⁵, P. Antonioli⁵², N. Apadula⁸¹, L. Aphecetche¹¹⁴, H. Appelshäuser⁶⁹, S. Arcelli²⁶, R. Arnaldi⁵⁷, O.W. Arnold^{105,35}, I.C. Arsene²⁰, M. Arslanodk¹⁰⁴, B. Audurier¹¹⁴, A. Augustinus³⁴, R. Averbeck¹⁰⁶, M.D. Azmi¹⁶, A. Badalà⁵⁴, Y.W. Baek^{77,59}, S. Bagnasco⁵⁷, R. Bailhache⁶⁹, R. Bala¹⁰¹, A. Baldisseri⁷⁴, M. Ball⁴⁴, R.C. Baral^{66,88}, A.M. Barbone²⁵, R. Barbera²⁷, F. Barile³², L. Barioglio²⁵, G.G. Barnaföldi¹⁴⁰, L.S. Barnby⁹³, V. Barret¹³¹, P. Bartalini⁷, K. Barth³⁴, E. Bartsch⁶⁹, N. Bastid¹³¹, S. Basu¹³⁹, G. Batigne¹¹⁴, B. Batyunya⁷⁶, P.C. Batzing²⁰, J.L. Bazo Alba¹¹¹, I.G. Bearden⁹¹, H. Beck¹⁰⁴, C. Bedda⁶², N.K. Behera⁵⁹, I. Belikov¹³³, F. Bellini^{34,26}, H. Bello Martinez², R. Bellwied¹²⁴, L.G.E. Beltran¹²⁰, V. Belyaev⁸², G. Bencedi¹⁴⁰, S. Beole²⁵, A. Bercuci⁸⁷, Y. Berdnikov⁹⁶, D. Berenyi¹⁴⁰, R.A. Bertens¹²⁷, D. Berzano^{57,34}, L. Betev³⁴, P.P. Bhaduri¹³⁷, A. Bhasin¹⁰¹, I.R. Bhat¹⁰¹, B. Bhattacharjee⁴³, J. Bhom¹¹⁸, A. Bianchi²⁵, L. Bianchi¹²⁴, N. Bianchi⁵⁰, C. Bianchin¹³⁹, J. Bielčik³⁸,

J. Bielčiková⁹⁴, A. Bilandzic^{35,105}, G. Biro¹⁴⁰, R. Biswas⁴, S. Biswas⁴, J.T. Blair¹¹⁹, D. Blau⁹⁰, C. Blume⁶⁹, G. Boca¹³⁴, F. Bock³⁴, A. Bogdanov⁸², L. Boldizsár¹⁴⁰, M. Bombara³⁹, G. Bonomi¹³⁵, M. Bonora³⁴, H. Borel⁷⁴, A. Borisso^{18,104}, M. Borri¹²⁶, E. Botta²⁵, C. Bourjau⁹¹, L. Bratrud⁶⁹, P. Braun-Munzinger¹⁰⁶, M. Bregant¹²¹, T.A. Broker⁶⁹, M. Broz³⁸, E.J. Brucken⁴⁵, E. Bruna⁵⁷, G.E. Bruno^{34,32}, D. Budnikov¹⁰⁸, H. Buesching⁶⁹, S. Bufalino³⁰, P. Buhler¹¹³, P. Buncic³⁴, O. Busch¹³⁰, Z. Buthelezi⁷⁵, J.B. Butt¹⁵, J.T. Buxton¹⁷, J. Cabala¹¹⁶, D. Caffarri^{34,92}, H. Caines¹⁴¹, A. Caliva^{106,62}, E. Calvo Villar¹¹¹, R.S. Camacho², P. Camerini²⁴, A.A. Capon¹¹³, F. Carena³⁴, W. Carena³⁴, F. Carnesecchi^{11,26}, J. Castillo Castellanos⁷⁴, A.J. Castro¹²⁷, E.A.R. Casula⁵³, C. Ceballos Sanchez⁹, S. Chandra¹³⁷, B. Chang¹²⁵, W. Chang⁷, S. Chapeland³⁴, M. Chartier¹²⁶, S. Chattopadhyay¹³⁷, S. Chattopadhyay¹⁰⁹, A. Chauvin^{105,35}, C. Cheshkov¹³², B. Cheynis¹³², V. Chibante Barroso³⁴, D.D. Chinellato¹²², S. Cho⁵⁹, P. Chochula³⁴, M. Chojnacki⁹¹, S. Choudhury¹³⁷, T. Chowdhury¹³¹, P. Christakoglou⁹², C.H. Christensen⁹¹, P. Christiansen³³, T. Chujo¹³⁰, S.U. Chung¹⁸, C. Cicalo⁵³, L. Cifarelli^{11,26}, F. Cindolo⁵², J. Cleymans¹⁰⁰, F. Colamaria^{51,32}, D. Colella^{64,34,51}, A. Collu⁸¹, M. Colocci²⁶, M. Concas^{57,ii}, G. Conesa Balbastre⁸⁰, Z. Conesa del Valle⁶⁰, J.G. Contreras³⁸, T.M. Cormier⁹⁵, Y. Corrales Morales⁵⁷, I. Cortés Maldonado², P. Cortese³¹, M.R. Cosentino¹²³, F. Costa³⁴, S. Costanza¹³⁴, J. Crkovská⁶⁰, P. Crochet¹³¹, E. Cuautle⁷¹, L. Cunqueiro^{70,95}, T. Dahms^{105,35}, A. Dainese⁵⁵, M.C. Danisch¹⁰⁴, A. Danu⁶⁷, D. Das¹⁰⁹, I. Das¹⁰⁹, S. Das⁴, A. Dash⁸⁸, S. Dash⁴⁷, S. De⁴⁸, A. De Caro²⁹, G. de Cataldo⁵¹, C. de Conti¹²¹, J. de Cuveland⁴¹, A. De Falco²³, D. De Gruttola^{29,11}, N. De Marco⁵⁷, S. De Pasquale²⁹, R.D. De Souza¹²², H.F. Degenhardt¹²¹, A. Deisting^{106,104}, A. Deloff⁸⁶, C. Deplano⁹², P. Dhankher⁴⁷, D. Di Bari³², A. Di Mauro³⁴, P. Di Nezza⁵⁰, B. Di Ruzza⁵⁵, T. Dietel¹⁰⁰, P. Dillenseger⁶⁹, Y. Ding⁷, R. Divià³⁴, Ø. Djuvsland²¹, A. Dobrin³⁴, D. Domenicis Gimenez¹²¹, B. Dönigus⁶⁹, O. Dordic²⁰, L.V.R. Doremalen⁶², A.K. Dubey¹³⁷, A. Dubla¹⁰⁶, L. Ducroux¹³², S. Dudi⁹⁹, A.K. Duggal⁹⁹, M. Dukhishyam⁸⁸, P. Dupieux¹³¹, R.J. Ehlers¹⁴¹, D. Elia⁵¹, E. Endress¹¹¹, H. Engel⁶⁸, E. Eppe¹⁴¹, B. Erasmus¹¹⁴, F. Erhardt⁹⁸, B. Espagnon⁶⁰, G. Eulisse³⁴, J. Eum¹⁸, D. Evans¹¹⁰, S. Evdokimov¹¹², L. Fabbietti^{105,35}, J. Favre⁸⁰, A. Fantoni⁵⁰, M. Fasel⁹⁵, L. Feldkamp⁷⁰, A. Feliciello⁵⁷, G. Feofilov¹³⁶, A. Fernández Téllez², A. Ferretti²⁵, A. Festanti^{28,34}, V.J.G. Feuillard^{74,131}, J. Figiel¹¹⁸, M.A.S. Figueredo¹²¹, S. Filchagin¹⁰⁸, D. Finogeev⁶¹, F.M. Fionda^{21,23}, M. Floris³⁴, S. Foertsch⁷⁵, P. Foka¹⁰⁶, S. Fokin⁹⁰, E. Fragiaco⁵⁸, A. Francescon³⁴, A. Francisco¹¹⁴, U. Frankendorf¹⁰⁶, G.G. Fronze²⁵, U. Fuchs³⁴, C. Furget⁸⁰, A. Furs⁶¹, M. Fusco Girard²⁹, J.J. Gaardhøje⁹¹, M. Gagliardi²⁵, A.M. Gago¹¹¹, K. Gajdosova⁹¹, M. Gallio²⁵, C.D. Galvan¹²⁰, P. Ganoti⁸⁵, C. Garabatos¹⁰⁶, E. Garcia-Solis¹², K. Garg²⁷, C. Gargiulo³⁴, P. Gasik^{105,35}, E.F. Gauger¹¹⁹, M.B. Gay Ducati⁷², M. Germain¹¹⁴, J. Ghosh¹⁰⁹, P. Ghosh¹³⁷, S.K. Ghosh⁴, P. Gianotti⁵⁰, P. Giubellino^{34,106,57}, P. Giubilato²⁸, E. Gladysz-Dziadus¹¹⁸, P. Glässel¹⁰⁴, D.M. Gómez Coral⁷³, A. Gomez Ramirez⁶⁸, A.S. Gonzalez³⁴, P. González-Zamora², S. Gorbunov⁴¹, L. Görlich¹¹⁸, S. Gotovac¹¹⁷, V. Grabski⁷³, L.K. Graczykowski¹³⁸, K.L. Graham¹¹⁰, L. Greiner⁸¹, A. Grelli⁶², C. Grigoras³⁴, V. Grigoriev⁸², A. Grigoryan¹, S. Grigoryan⁷⁶, J.M. Gronefeld¹⁰⁶, F. Groa³⁰, J.F. Grosse-Oetringhaus³⁴, R. Grosso¹⁰⁶, F. Guber⁶¹, R. Guernane⁸⁰, B. Guerzoni²⁶, M. Guittiere¹¹⁴, K. Gulbrandsen⁹¹, T. Gunji¹²⁹, A. Gupta¹⁰¹, R. Gupta¹⁰¹, I.B. Guzman², R. Haake³⁴, C. Hadjidakis⁶⁰, H. Hamagaki⁸³, G. Hamar¹⁴⁰, J.C. Hamon¹³³, M.R. Haque⁶², J.W. Harris¹⁴¹, A. Harton¹², H. Hassan⁸⁰, D. Hatzifotiadou^{52,11}, S. Hayashi¹²⁹, S.T. Heckel⁶⁹, E. Hellbär⁶⁹, H. Helstrup³⁶, A. Herghelegiu⁸⁷, E.G. Hernandez², G. Herrera Corral¹⁰, F. Herrmann⁷⁰, B.A. Hess¹⁰³, K.F. Hetland³⁶, H. Hillemanns³⁴, C. Hills¹²⁶, B. Hippolyte¹³³, B. Hohlweger¹⁰⁵, D. Horak³⁸, S. Hornung¹⁰⁶, R. Hosokawa^{80,130}, P. Hristov³⁴, C. Hughes¹²⁷, T.J. Humanic¹⁷, N. Hussain⁴³, T. Hussain¹⁶, D. Hutter⁴¹, D.S. Hwang¹⁹, J.P. Iddon¹²⁶, S.A. Iga Buitron⁷¹, R. Ilkaev¹⁰⁸, M. Inaba¹³⁰, M. Ippolitov^{82,90}, M.S. Islam¹⁰⁹, M. Ivanov¹⁰⁶, V. Ivanov⁹⁶, V. Izucheev¹¹², B. Jacak⁸¹, N. Jacazio²⁶, P.M. Jacobs⁸¹, M.B. Jadhav⁴⁷, S. Jadlovská¹¹⁶, J. Jadlovsky¹¹⁶, S. Jaelani⁶², C. Jahnke³⁵, M.J. Jakubowska¹³⁸, M.A. Janik¹³⁸, P.H.S.Y. Jayarathna¹²⁴, C. Jena⁸⁸, M. Jercic⁹⁸, R.T. Jimenez Bustamante¹⁰⁶, P.G. Jones¹¹⁰, A. Jusko¹¹⁰, P. Kalinak⁶⁴, A. Kalweit³⁴, J.H. Kang¹⁴², V. Kaplin⁸², S. Kar¹³⁷, A. Karasu Uysal⁷⁹, O. Karavichev⁶¹, T. Karavicheva⁶¹, L. Karayan^{106,104}, P. Karczmarczyk³⁴, E. Karpechev⁶¹, U. Keschull⁶⁸, R. Keidel¹⁴³, D.L.D. Keijdener⁶², M. Keil³⁴, B. Ketzer⁴⁴, Z. Khabanova⁹², P. Khan¹⁰⁹, S. Khan¹⁶, S.A. Khan¹³⁷, A. Khanzadeev⁹⁶, Y. Kharlov¹¹², A. Khatun¹⁶, A. Khuntia⁴⁸, M.M. Kielbowicz¹¹⁸, B. Kileng³⁶, B. Kim¹³⁰, D. Kim¹⁴², D.J. Kim¹²⁵, E.J. Kim¹⁴, H. Kim¹⁴², J.S. Kim⁴², J. Kim¹⁰⁴, M. Kim⁵⁹, S. Kim¹⁹, T. Kim¹⁴², S. Kirsch⁴¹, I. Kisel⁴¹, S. Kiselev⁶³, A. Kisel¹³⁸, G. Kiss¹⁴⁰, J.L. Klay⁶, C. Klein⁶⁹, J. Klein³⁴, C. Klein-Bösing⁷⁰,

S. Klewin¹⁰⁴, A. Kluge³⁴, M.L. Knichel^{104,34}, A.G. Knospe¹²⁴, C. Kobdaj¹¹⁵, M. Kofarago¹⁴⁰, M.K. Köhler¹⁰⁴, T. Kollegger¹⁰⁶, V. Kondratiev¹³⁶, N. Kondratyeva⁸², E. Kondratyuk¹¹², A. Konevskikh⁶¹, M. Konyushikhin¹³⁹, M. Kopicik¹¹⁶, M. Kour¹⁰¹, C. Kouzinopoulos³⁴, O. Kovalenko⁸⁶, V. Kovalenko¹³⁶, M. Kowalski¹¹⁸, I. Králik⁶⁴, A. Kravčáková³⁹, L. Kreis¹⁰⁶, M. Krivda^{110,64}, F. Krizek⁹⁴, E. Kryshen⁹⁶, M. Krzewicki⁴¹, A.M. Kubera¹⁷, V. Kučera⁹⁴, C. Kuhn¹³³, P.G. Kuijer⁹², A. Kumar¹⁰¹, J. Kumar⁴⁷, L. Kumar⁹⁹, S. Kumar⁴⁷, S. Kundu⁸⁸, P. Kurashvili⁸⁶, A. Kurepin⁶¹, A.B. Kurepin⁶¹, A. Kuryakin¹⁰⁸, S. Kushpil⁹⁴, M.J. Kweon⁵⁹, Y. Kwon¹⁴², S.L. La Pointe⁴¹, P. La Rocca²⁷, C. Lagana Fernandes¹²¹, Y.S. Lai⁸¹, I. Lakomov³⁴, R. Langoy⁴⁰, K. Lapidus¹⁴¹, C. Lara⁶⁸, A. Lardeux²⁰, A. Lattuca²⁵, E. Laudi³⁴, R. Lavicka³⁸, R. Lea²⁴, L. Leardini¹⁰⁴, S. Lee¹⁴², F. Lehas⁹², S. Lehner¹¹³, J. Lehrbach⁴¹, R.C. Lemmon⁹³, E. Leogrande⁶², I. León Monzón¹²⁰, P. Lévai¹⁴⁰, X. Li¹³, X.L. Li⁷, J. Lien⁴⁰, R. Lietava¹¹⁰, B. Lim¹⁸, S. Lindal²⁰, V. Lindenstruth⁴¹, S.W. Lindsay¹²⁶, C. Lippmann¹⁰⁶, M.A. Lisa¹⁷, V. Litichevskiy⁴⁵, A. Liu⁸¹, W.J. Llope¹³⁹, D.F. Lodato⁶², P.I. Loenne²¹, V. Loginov⁸², C. Loizides^{81,95}, P. Loncar¹¹⁷, X. Lopez¹³¹, E. López Torres⁹, A. Lowe¹⁴⁰, P. Luettig⁶⁹, J.R. Luhder⁷⁰, M. Lunardon²⁸, G. Luparello^{24,58}, M. Lupi³⁴, T.H. Lutz¹⁴¹, A. Maevskaya⁶¹, M. Mager³⁴, S.M. Mahmood²⁰, A. Maire¹³³, R.D. Majka¹⁴¹, M. Malaev⁹⁶, L. Malinina^{76,iii}, D. Mal'Kevich⁶³, P. Malzacher¹⁰⁶, A. Mamonov¹⁰⁸, V. Manko⁹⁰, F. Manso¹³¹, V. Manzari⁵¹, Y. Mao⁷, M. Marchisone^{132,128,75}, J. Mareš⁶⁵, G.V. Margagliotti²⁴, A. Margotti⁵², J. Margutti⁶², A. Marín¹⁰⁶, C. Markert¹¹⁹, M. Marquard⁶⁹, N.A. Martin¹⁰⁶, P. Martinengo³⁴, J.A.L. Martinez⁶⁸, M.I. Martínez², G. Martínez García¹¹⁴, M. Martinez Pedreira³⁴, S. Masciocchi¹⁰⁶, M. Maserà²⁵, A. Masoni⁵³, L. Massacrier⁶⁰, E. Masson¹¹⁴, A. Mastroserio⁵¹, A.M. Mathis^{35,105}, P.F.T. Matuoka¹²¹, A. Matyja¹²⁷, C. Mayer¹¹⁸, J. Mazer¹²⁷, M. Mazzilli³², M.A. Mazzoni⁵⁶, F. Meddi²², Y. Melikyan⁸², A. Menchaca-Rocha⁷³, E. Meninno²⁹, J. Mercado Pérez¹⁰⁴, M. Meres³⁷, S. Mhlanga¹⁰⁰, Y. Miake¹³⁰, M.M. Mieskolainen⁴⁵, D.L. Mihaylov¹⁰⁵, K. Mikhaylov^{63,76}, A. Mischke⁶², A.N. Mishra⁴⁸, D. Miśkowiec¹⁰⁶, J. Mitra¹³⁷, C.M. Mitu⁶⁷, N. Mohammadi^{34,62}, A.P. Mohanty⁶², B. Mohanty⁸⁸, M. Mohisin Khan^{16,iv}, D.A. Moreira De Godoy⁷⁰, L.A.P. Moreno², S. Moretto²⁸, A. Morreale¹¹⁴, A. Morsch³⁴, V. Muccifora⁵⁰, E. Mudnic¹¹⁷, D. Mühlheim⁷⁰, S. Muhuri¹³⁷, M. Mukherjee⁴, J.D. Mulligan¹⁴¹, M.G. Munhoz¹²¹, K. Munning⁴⁴, M.I.A. Munoz⁸¹, R.H. Munzer⁶⁹, H. Murakami¹²⁹, S. Murray⁷⁵, L. Musa³⁴, J. Musinsky⁶⁴, C.J. Myers¹²⁴, J.W. Myrcha¹³⁸, D. Nag⁴, B. Naik⁴⁷, R. Nair⁸⁶, B.K. Nandi⁴⁷, R. Nania^{11,52}, E. Nappi⁵¹, A. Narayan⁴⁷, M.U. Naru¹⁵, H. Natal da Luz¹²¹, C. Nattress¹²⁷, S.R. Navarro², K. Nayak⁸⁸, R. Nayak⁴⁷, T.K. Nayak¹³⁷, S. Nazarenko¹⁰⁸, R.A. Negrao De Oliveira^{69,34}, L. Nellen⁷¹, S.V. Nesbo³⁶, G. Neskovic⁴¹, F. Ng¹²⁴, M. Nicassio¹⁰⁶, M. Niculescu⁶⁷, J. Niedziela^{138,34}, B.S. Nielsen⁹¹, S. Nikolaev⁹⁰, S. Nikulin⁹⁰, V. Nikulin⁹⁶, A. Nobuhiro⁴⁶, F. Noferini^{11,52}, P. Nomokonov⁷⁶, G. Nooren⁶², J.C.C. Noris², J. Norman^{126,80}, A. Nyanin⁹⁰, J. Nystrand²¹, H. Oeschler^{18,104,i}, H. Oh¹⁴², A. Ohlson¹⁰⁴, L. Olah¹⁴⁰, J. Oleniacz¹³⁸, A.C. Oliveira Da Silva¹²¹, M.H. Oliver¹⁴¹, J. Onderwaater¹⁰⁶, C. Oppedisano⁵⁷, R. Orava⁴⁵, M. Oravec¹¹⁶, A. Ortiz Velasquez⁷¹, A. Oskarsson³³, J. Otwinowski¹¹⁸, K. Oyama⁸³, Y. Pachmayer¹⁰⁴, V. Pacik⁹¹, D. Pagano¹³⁵, G. Paić⁷¹, P. Palni⁷, J. Pan¹³⁹, A.K. Pandey⁴⁷, S. Panebianco⁷⁴, V. Papikyan¹, P. Pareek⁴⁸, J. Park⁵⁹, S. Parmar⁹⁹, A. Passfeld⁷⁰, S.P. Pathak¹²⁴, R.N. Patra¹³⁷, B. Paul⁵⁷, H. Pei⁷, T. Peitzmann⁶², X. Peng⁷, L.G. Pereira⁷², H. Pereira Da Costa⁷⁴, D. Peresunko^{82,90}, E. Perez Lezama⁶⁹, V. Peskov⁶⁹, Y. Pestov⁵, V. Petráček³⁸, M. Petrovici⁸⁷, C. Petta²⁷, R.P. Pezzi⁷², S. Piano⁵⁸, M. Pikna³⁷, P. Pillot¹¹⁴, L.O.D.L. Pimentel⁹¹, O. Pinazza^{52,34}, L. Pinsky¹²⁴, D.B. Piyarathna¹²⁴, M. Płoskoń⁸¹, M. Planinic⁹⁸, F. Pliquett⁶⁹, J. Pluta¹³⁸, S. Pochybova¹⁴⁰, P.L.M. Podesta-Lerma¹²⁰, M.G. Poghosyan⁹⁵, B. Polichtchouk¹¹², N. Poljak⁹⁸, W. Poonsawat¹¹⁵, A. Pop⁸⁷, H. Poppenborg⁷⁰, S. Porteboeuf-Houssais¹³¹, V. Pozdniakov⁷⁶, S.K. Prasad⁴, R. Preghenella⁵², F. Prino⁵⁷, C.A. Pruneau¹³⁹, I. Pshenichnov⁶¹, M. Puccio²⁵, V. Punin¹⁰⁸, J. Putschke¹³⁹, S. Raha⁴, S. Rajput¹⁰¹, J. Rak¹²⁵, A. Rakotozafindrabe⁷⁴, L. Ramello³¹, F. Rami¹³³, D.B. Rana¹²⁴, R. Raniwala¹⁰², S. Raniwala¹⁰², S.S. Räsänen⁴⁵, B.T. Rascanu⁶⁹, D. Rathee⁹⁹, V. Ratza⁴⁴, I. Ravasenga³⁰, K.F. Read^{127,95}, K. Redlich^{86,v}, A. Rehman²¹, P. Reichelt⁶⁹, F. Reidt³⁴, X. Ren⁷, R. Renfordt⁶⁹, A. Reshetin⁶¹, K. Reygers¹⁰⁴, V. Riabov⁹⁶, T. Richert^{62,33}, M. Richter²⁰, P. Riedler³⁴, W. Riegler³⁴, F. Riggi²⁷, C. Ristea⁶⁷, M. Rodríguez Cahuantzi², K. Røed²⁰, R. Rogalev¹¹², E. Rogochaya⁷⁶, D. Rohr^{34,41}, D. Röhrich²¹, P.S. Rokita¹³⁸, F. Ronchetti⁵⁰, E.D. Rosas⁷¹, K. Roslon¹³⁸, P. Rosnet¹³¹, A. Rossi^{55,28}, A. Rotondi¹³⁴, F. Roukoutakis⁸⁵, C. Roy¹³³, P. Roy¹⁰⁹, O.V. Rueda⁷¹, R. Rui²⁴, B. Romyantsev⁷⁶, A. Rustamov⁸⁹, E. Ryabinkin⁹⁰, Y. Ryabov⁹⁶, A. Rybicki¹¹⁸, S. Saarinen⁴⁵, S. Sadhu¹³⁷, S. Sadovsky¹¹², K. Šafařík³⁴, S.K. Saha¹³⁷, B. Sahoo⁴⁷, P. Sahoo⁴⁸, R. Sahoo⁴⁸, S. Sahoo⁶⁶, P.K. Sahu⁶⁶, J. Saini¹³⁷,

S. Sakai¹³⁰, M.A. Saleh¹³⁹, J. Salzwedel¹⁷, S. Sambyal¹⁰¹, V. Samsonov^{96,82}, A. Sandoval⁷³, A. Sarkar⁷⁵, D. Sarkar¹³⁷, N. Sarkar¹³⁷, P. Sarma⁴³, M.H.P. Sas⁶², E. Scapparone⁵², F. Scarlassara²⁸, B. Schaefer⁹⁵, H.S. Scheid⁶⁹, C. Schiaua⁸⁷, R. Schicker¹⁰⁴, C. Schmidt¹⁰⁶, H.R. Schmidt¹⁰³, M.O. Schmidt¹⁰⁴, M. Schmidt¹⁰³, N.V. Schmidt^{95,69}, J. Schukraft³⁴, Y. Schutz^{34,133}, K. Schwarz¹⁰⁶, K. Schweda¹⁰⁶, G. Scioli²⁶, E. Scomparin⁵⁷, M. Šefčík³⁹, J.E. Seger⁹⁷, Y. Sekiguchi¹²⁹, D. Sekihata⁴⁶, I. Selyuzhenkov^{106,82}, K. Senosi⁷⁵, S. Senyukov¹³³, E. Serradilla⁷³, P. Sett⁴⁷, A. Sevcenco⁶⁷, A. Shabanov⁶¹, A. Shabetai¹¹⁴, R. Shahoyan³⁴, W. Shaikh¹⁰⁹, A. Shangaraev¹¹², A. Sharma⁹⁹, A. Sharma¹⁰¹, M. Sharma¹⁰¹, M. Sharma¹⁰¹, N. Sharma⁹⁹, A.I. Sheikh¹³⁷, K. Shigaki⁴⁶, M. Shimomura⁸⁴, S. Shirinkin⁶³, Q. Shou⁷, K. Shtejer^{9,25}, Y. Sibiriak⁹⁰, S. Siddhanta⁵³, K.M. Sielewicz³⁴, T. Siemiarczuk⁸⁶, S. Silaeva⁹⁰, D. Silvermyr³³, G. Simatovic^{92,98}, G. Simonetti³⁴, R. Singaraju¹³⁷, R. Singh⁸⁸, V. Singhal¹³⁷, T. Sinha¹⁰⁹, B. Sitar³⁷, M. Sitta³¹, T.B. Skaali²⁰, M. Slupecki¹²⁵, N. Smirnov¹⁴¹, R.J.M. Snellings⁶², T.W. Snellman¹²⁵, J. Song¹⁸, F. Soramel²⁸, S. Sorensen¹²⁷, F. Sozzi¹⁰⁶, I. Sputowska¹¹⁸, J. Stachel¹⁰⁴, I. Stan⁶⁷, P. Stankus⁹⁵, E. Stenlund³³, D. Stocco¹¹⁴, M.M. Stortvedt³⁶, P. Strmen³⁷, A.A.P. Suaide¹²¹, T. Sugitate⁴⁶, C. Suires⁶⁰, M. Suleymanov¹⁵, M. Suljic²⁴, R. Sultanov⁶³, M. Šumbera⁹⁴, S. Sumowidagdo⁴⁹, K. Suzuki¹¹³, S. Swain⁶⁶, A. Szabo³⁷, I. Szarka³⁷, U. Tabassam¹⁵, J. Takahashi¹²², G.J. Tambave²¹, N. Tanaka¹³⁰, M. Tarhini^{114,60}, M. Tariq¹⁶, M.G. Tarzila⁸⁷, A. Tauro³⁴, G. Tejeda Muñoz², A. Telesca³⁴, K. Terasaki¹²⁹, C. Terrevoli²⁸, B. Teyssier¹³², D. Thakur⁴⁸, S. Thakur¹³⁷, D. Thomas¹¹⁹, F. Thoresen⁹¹, R. Tieulent¹³², A. Tikhonov⁶¹, A.R. Timmins¹²⁴, A. Toia⁶⁹, M. Toppi⁵⁰, S.R. Torres¹²⁰, S. Tripathy⁴⁸, S. Trogolo²⁵, G. Trombetta³², L. Tropp³⁹, V. Trubnikov³, W.H. Trzaska¹²⁵, B.A. Trzeciak⁶², T. Tsuji¹²⁹, A. Tumkin¹⁰⁸, R. Turrisi⁵⁵, T.S. Tveter²⁰, K. Ullaland²¹, E.N. Umaka¹²⁴, A. Uras¹³², G.L. Usai²³, A. Utrobicic⁹⁸, M. Vala^{116,64}, J. Van Der Maarel⁶², J.W. Van Hoorne³⁴, M. van Leeuwen⁶², T. Vanat⁹⁴, P. Vande Vyvre³⁴, D. Varga¹⁴⁰, A. Vargas², M. Vargyas¹²⁵, R. Varma⁴⁷, M. Vasileiou⁸⁵, A. Vasiliev⁹⁰, A. Vauthier⁸⁰, O. Vázquez Doce^{105,35}, V. Vechernin¹³⁶, A.M. Veen⁶², A. Velure²¹, E. Vercellin²⁵, S. Vergara Limón², L. Vermunt⁶², R. Vernet⁸, R. Vértesi¹⁴⁰, L. Vickovic¹¹⁷, J. Viinikainen¹²⁵, Z. Vilakazi¹²⁸, O. Villalobos Baillie¹¹⁰, A. Villatoro Tello², A. Vinogradov⁹⁰, L. Vinogradov¹³⁶, T. Virgili²⁹, V. Vislavicius³³, A. Vodopyanov⁷⁶, M.A. Völkl¹⁰³, K. Voloshin⁶³, S.A. Voloshin¹³⁹, G. Volpe³², B. von Haller³⁴, I. Vorobyev^{105,35}, D. Voscek¹¹⁶, D. Vranic^{34,106}, J. Vrláková³⁹, B. Wagner²¹, H. Wang⁶², M. Wang⁷, Y. Watanabe^{129,130}, M. Weber¹¹³, S.G. Weber¹⁰⁶, A. Wegrzynek³⁴, D.F. Weiser¹⁰⁴, S.C. Wenzel³⁴, J.P. Wessels⁷⁰, U. Westerhoff⁷⁰, A.M. Whitehead¹⁰⁰, J. Wiechula⁶⁹, J. Wikne²⁰, G. Wilk⁸⁶, J. Wilkinson⁵², G.A. Willems^{70,34}, M.C.S. Williams⁵², E. Willsher¹¹⁰, B. Windelband¹⁰⁴, W.E. Witt¹²⁷, R. Xu⁷, S. Yalcin⁷⁹, K. Yamakawa⁴⁶, P. Yang⁷, S. Yano⁴⁶, Z. Yin⁷, H. Yokoyama^{80,130}, I.-K. Yoo¹⁸, J.H. Yoon⁵⁹, E. Yun¹⁸, V. Yurchenko³, V. Zaccolo⁵⁷, A. Zaman¹⁵, C. Zampolli³⁴, H.J.C. Zanoli¹²¹, N. Zardoshti¹¹⁰, A. Zarochentsev¹³⁶, P. Závada⁶⁵, N. Zaviyalov¹⁰⁸, H. Zbroszczyk¹³⁸, M. Zhalov⁹⁶, H. Zhang^{7,21}, X. Zhang⁷, Y. Zhang⁷, C. Zhang⁶², Z. Zhang^{131,7}, C. Zhao²⁰, N. Zhigareva⁶³, D. Zhou⁷, Y. Zhou⁹¹, Z. Zhou²¹, H. Zhu²¹, J. Zhu⁷, Y. Zhu⁷, A. Zichichi^{26,11}, M.B. Zimmermann³⁴, G. Zinovjev³, J. Zmeskal¹¹³, S. Zou⁷

¹ A.I. Alikhanyan National Science Laboratory (Yerevan Physics Institute) Foundation, Yerevan, Armenia

² Benemérita Universidad Autónoma de Puebla, Puebla, Mexico

³ Bogolyubov Institute for Theoretical Physics, Kiev, Ukraine

⁴ Bose Institute, Department of Physics and Centre for Astroparticle Physics and Space Science (CAPSS), Kolkata, India

⁵ Budker Institute for Nuclear Physics, Novosibirsk, Russia

⁶ California Polytechnic State University, San Luis Obispo, CA, United States

⁷ Central China Normal University, Wuhan, China

⁸ Centre de Calcul de l'IN2P3, Villeurbanne, Lyon, France

⁹ Centro de Aplicaciones Tecnológicas y Desarrollo Nuclear (CEADEN), Havana, Cuba

¹⁰ Centro de Investigación y de Estudios Avanzados (CINVESTAV), Mexico City and Mérida, Mexico

¹¹ Centro Fermi – Museo Storico della Fisica e Centro Studi e Ricerche “Enrico Fermi”, Rome, Italy

¹² Chicago State University, Chicago, IL, United States

¹³ China Institute of Atomic Energy, Beijing, China

¹⁴ Chonbuk National University, Jeonju, Republic of Korea

¹⁵ COMSATS Institute of Information Technology (CIIT), Islamabad, Pakistan

¹⁶ Department of Physics, Aligarh Muslim University, Aligarh, India

¹⁷ Department of Physics, Ohio State University, Columbus, OH, United States

¹⁸ Department of Physics, Pusan National University, Pusan, Republic of Korea

¹⁹ Department of Physics, Sejong University, Seoul, Republic of Korea

²⁰ Department of Physics, University of Oslo, Oslo, Norway

²¹ Department of Physics and Technology, University of Bergen, Bergen, Norway

²² Dipartimento di Fisica dell'Università ‘La Sapienza’ and Sezione INFN, Rome, Italy

²³ Dipartimento di Fisica dell'Università and Sezione INFN, Cagliari, Italy

²⁴ Dipartimento di Fisica dell'Università and Sezione INFN, Trieste, Italy

- 25 Dipartimento di Fisica dell'Università and Sezione INFN, Turin, Italy
- 26 Dipartimento di Fisica e Astronomia dell'Università and Sezione INFN, Bologna, Italy
- 27 Dipartimento di Fisica e Astronomia dell'Università and Sezione INFN, Catania, Italy
- 28 Dipartimento di Fisica e Astronomia dell'Università and Sezione INFN, Padova, Italy
- 29 Dipartimento di Fisica 'E.R. Caianiello' dell'Università and Gruppo Collegato INFN, Salerno, Italy
- 30 Dipartimento DISAT del Politecnico and Sezione INFN, Turin, Italy
- 31 Dipartimento di Scienze e Innovazione Tecnologica dell'Università del Piemonte Orientale and INFN Sezione di Torino, Alessandria, Italy
- 32 Dipartimento Interateneo di Fisica 'M. Merlin' and Sezione INFN, Bari, Italy
- 33 Division of Experimental High Energy Physics, University of Lund, Lund, Sweden
- 34 European Organization for Nuclear Research (CERN), Geneva, Switzerland
- 35 Excellence Cluster Universe, Technische Universität München, Munich, Germany
- 36 Faculty of Engineering, Bergen University College, Bergen, Norway
- 37 Faculty of Mathematics, Physics and Informatics, Comenius University, Bratislava, Slovakia
- 38 Faculty of Nuclear Sciences and Physical Engineering, Czech Technical University in Prague, Prague, Czech Republic
- 39 Faculty of Science, P.J. Šafárik University, Košice, Slovakia
- 40 Faculty of Technology, Buskerud and Vestfold University College, Tonsberg, Norway
- 41 Frankfurt Institute for Advanced Studies, Johann Wolfgang Goethe-Universität Frankfurt, Frankfurt, Germany
- 42 Gangneung-Wonju National University, Gangneung, Republic of Korea
- 43 Gauhati University, Department of Physics, Guwahati, India
- 44 Helmholtz-Institut für Strahlen- und Kernphysik, Rheinische Friedrich-Wilhelms-Universität Bonn, Bonn, Germany
- 45 Helsinki Institute of Physics (HIP), Helsinki, Finland
- 46 Hiroshima University, Hiroshima, Japan
- 47 Indian Institute of Technology Bombay (IIT), Mumbai, India
- 48 Indian Institute of Technology Indore, Indore, India
- 49 Indonesian Institute of Sciences, Jakarta, Indonesia
- 50 INFN, Laboratori Nazionali di Frascati, Frascati, Italy
- 51 INFN, Sezione di Bari, Bari, Italy
- 52 INFN, Sezione di Bologna, Bologna, Italy
- 53 INFN, Sezione di Cagliari, Cagliari, Italy
- 54 INFN, Sezione di Catania, Catania, Italy
- 55 INFN, Sezione di Padova, Padova, Italy
- 56 INFN, Sezione di Roma, Rome, Italy
- 57 INFN, Sezione di Torino, Turin, Italy
- 58 INFN, Sezione di Trieste, Trieste, Italy
- 59 Inha University, Incheon, Republic of Korea
- 60 Institut de Physique Nucléaire d'Orsay (IPNO), Université Paris-Sud, CNRS-IN2P3, Orsay, France
- 61 Institute for Nuclear Research, Academy of Sciences, Moscow, Russia
- 62 Institute for Subatomic Physics of Utrecht University, Utrecht, Netherlands
- 63 Institute for Theoretical and Experimental Physics, Moscow, Russia
- 64 Institute of Experimental Physics, Slovak Academy of Sciences, Košice, Slovakia
- 65 Institute of Physics, Academy of Sciences of the Czech Republic, Prague, Czech Republic
- 66 Institute of Physics, Bhubaneswar, India
- 67 Institute of Space Science (ISS), Bucharest, Romania
- 68 Institut für Informatik, Johann Wolfgang Goethe-Universität Frankfurt, Frankfurt, Germany
- 69 Institut für Kernphysik, Johann Wolfgang Goethe-Universität Frankfurt, Frankfurt, Germany
- 70 Institut für Kernphysik, Westfälische Wilhelms-Universität Münster, Münster, Germany
- 71 Instituto de Ciencias Nucleares, Universidad Nacional Autónoma de México, Mexico City, Mexico
- 72 Instituto de Física, Universidade Federal do Rio Grande do Sul (UFRGS), Porto Alegre, Brazil
- 73 Instituto de Física, Universidad Nacional Autónoma de México, Mexico City, Mexico
- 74 IRFU, CEA, Université Paris-Saclay, Saclay, France
- 75 iThemba LABS, National Research Foundation, Somerset West, South Africa
- 76 Joint Institute for Nuclear Research (JINR), Dubna, Russia
- 77 Konkuk University, Seoul, Republic of Korea
- 78 Korea Institute of Science and Technology Information, Daejeon, Republic of Korea
- 79 KTO Karatay University, Konya, Turkey
- 80 Laboratoire de Physique Subatomique et de Cosmologie, Université Grenoble-Alpes, CNRS-IN2P3, Grenoble, France
- 81 Lawrence Berkeley National Laboratory, Berkeley, CA, United States
- 82 Moscow Engineering Physics Institute, Moscow, Russia
- 83 Nagasaki Institute of Applied Science, Nagasaki, Japan
- 84 Nara Women's University (NWU), Nara, Japan
- 85 National and Kapodistrian University of Athens, Physics Department, Athens, Greece
- 86 National Centre for Nuclear Studies, Warsaw, Poland
- 87 National Institute for Physics and Nuclear Engineering, Bucharest, Romania
- 88 National Institute of Science Education and Research, HBNI, Jatni, India
- 89 National Nuclear Research Center, Baku, Azerbaijan
- 90 National Research Centre Kurchatov Institute, Moscow, Russia
- 91 Niels Bohr Institute, University of Copenhagen, Copenhagen, Denmark
- 92 Nikhef, Nationaal instituut voor subatomaire fysica, Amsterdam, Netherlands
- 93 Nuclear Physics Group, STFC Daresbury Laboratory, Daresbury, United Kingdom
- 94 Nuclear Physics Institute, Academy of Sciences of the Czech Republic, Řež u Prahy, Czech Republic
- 95 Oak Ridge National Laboratory, Oak Ridge, TN, United States
- 96 Petersburg Nuclear Physics Institute, Gatchina, Russia
- 97 Physics Department, Creighton University, Omaha, NE, United States
- 98 Physics department, Faculty of science, University of Zagreb, Zagreb, Croatia
- 99 Physics Department, Panjab University, Chandigarh, India
- 100 Physics Department, University of Cape Town, Cape Town, South Africa
- 101 Physics Department, University of Jammu, Jammu, India
- 102 Physics Department, University of Rajasthan, Jaipur, India
- 103 Physikalisches Institut, Eberhard Karls Universität Tübingen, Tübingen, Germany

- ¹⁰⁴ Physikalisches Institut, Ruprecht-Karls-Universität Heidelberg, Heidelberg, Germany
¹⁰⁵ Physik Department, Technische Universität München, Munich, Germany
¹⁰⁶ Research Division and ExtreMe Matter Institute EMMI, GSI Helmholtzzentrum für Schwerionenforschung GmbH, Darmstadt, Germany
¹⁰⁷ Rudjer Bošković Institute, Zagreb, Croatia
¹⁰⁸ Russian Federal Nuclear Center (VNIIEF), Sarov, Russia
¹⁰⁹ Saha Institute of Nuclear Physics, Kolkata, India
¹¹⁰ School of Physics and Astronomy, University of Birmingham, Birmingham, United Kingdom
¹¹¹ Sección Física, Departamento de Ciencias, Pontificia Universidad Católica del Perú, Lima, Peru
¹¹² SSC IHEP of NRC Kurchatov institute, Protvino, Russia
¹¹³ Stefan Meyer Institut für Subatomare Physik (SMI), Vienna, Austria
¹¹⁴ SUBATECH, IMT Atlantique, Université de Nantes, CNRS-IN2P3, Nantes, France
¹¹⁵ Suranaree University of Technology, Nakhon Ratchasima, Thailand
¹¹⁶ Technical University of Košice, Košice, Slovakia
¹¹⁷ Technical University of Split FESB, Split, Croatia
¹¹⁸ The Henryk Niewodniczanski Institute of Nuclear Physics, Polish Academy of Sciences, Cracow, Poland
¹¹⁹ The University of Texas at Austin, Austin, TX, United States
¹²⁰ Universidad Autónoma de Sinaloa, Culiacán, Mexico
¹²¹ Universidade de São Paulo (USP), São Paulo, Brazil
¹²² Universidade Estadual de Campinas (UNICAMP), Campinas, Brazil
¹²³ Universidade Federal do ABC, Santo Andre, Brazil
¹²⁴ University of Houston, Houston, TX, United States
¹²⁵ University of Jyväskylä, Jyväskylä, Finland
¹²⁶ University of Liverpool, Liverpool, United Kingdom
¹²⁷ University of Tennessee, Knoxville, TN, United States
¹²⁸ University of the Witwatersrand, Johannesburg, South Africa
¹²⁹ University of Tokyo, Tokyo, Japan
¹³⁰ University of Tsukuba, Tsukuba, Japan
¹³¹ Université Clermont Auvergne, CNRS/IN2P3, LPC, Clermont-Ferrand, France
¹³² Université de Lyon, Université Lyon 1, CNRS/IN2P3, IPN-Lyon, Villeurbanne, Lyon, France
¹³³ Université de Strasbourg, CNRS, IPHC UMR 7178, F-67000 Strasbourg, France
¹³⁴ Università degli Studi di Pavia, Pavia, Italy
¹³⁵ Università di Brescia, Brescia, Italy
¹³⁶ V. Fock Institute for Physics, St. Petersburg State University, St. Petersburg, Russia
¹³⁷ Variable Energy Cyclotron Centre, Kolkata, India
¹³⁸ Warsaw University of Technology, Warsaw, Poland
¹³⁹ Wayne State University, Detroit, MI, United States
¹⁴⁰ Wigner Research Centre for Physics, Hungarian Academy of Sciences, Budapest, Hungary
¹⁴¹ Yale University, New Haven, CT, United States
¹⁴² Yonsei University, Seoul, Republic of Korea
¹⁴³ Zentrum für Technologietransfer und Telekommunikation (ZTT), Fachhochschule Worms, Worms, Germany

i Deceased.

ii Dipartimento DET del Politecnico di Torino, Turin, Italy.

iii M.V. Lomonosov Moscow State University, D.V. Skobeltsyn Institute of Nuclear, Physics, Moscow, Russia.

iv Department of Applied Physics, Aligarh Muslim University, Aligarh, India.

v Institute of Theoretical Physics, University of Wrocław, Poland.